Available online at www.sciencedirect.com
SCIENCE DIRECT®
Biochemical and Biophysical Research Communications 309 (2003) 923–928
BBRC
www.elsevier.com/locate/ybbrc

Docking and small angle X-ray scattering studies of purine nucleoside phosphorylase

Walter Filgueira de Azevedo Jr.,[a,b,*] Giovanni César dos Santos,[a] Denis Marangoni dos Santos,[a] Johnny Rizzieri Olivieri,[a,b] Fernanda Canduri,[a,b] Rafael Guimarães Silva,[c] Luiz Augusto Basso,[c] Gaby Renard,[c] Isabel Osório da Fonseca,[c] Maria Anita Mendes,[b,d] Mário Sérgio Palma,[b,d] and Diógenes Santiago Santos[c]

[a] *Departamento de Física, UNESP, São José do Rio Preto, SP 15054-000, Brazil*
[b] *Center for Applied Toxinology, Instituto Butantan, São Paulo, SP 05503-900, Brazil*
[c] *Rede Brasileira de Pesquisas em Tuberculose, Departamento de Biologia Molecular e Biotecnologia, UFRGS, Porto Alegre, RS 91501-970, Brazil*
[d] *Laboratory of Structural Biology and Zoochemistry, Department of Biology, Institute of Biosciences, UNESP, Rio Claro, SP 13506-900, Brazil*

Received 19 August 2003

Abstract

Docking simulations have been used to assess protein complexes with some success. Small angle X-ray scattering (SAXS) is a well-established technique to investigate protein spatial configuration. This work describes the integration of geometric docking with SAXS to investigate the quaternary structure of recombinant human purine nucleoside phosphorylase (PNP). This enzyme catalyzes the reversible phosphorolysis of *N*-ribosidic bonds of purine nucleosides and deoxynucleosides. A genetic deficiency due to mutations in the gene encoding for PNP causes gradual decrease in T-cell immunity. Inappropriate activation of T-cells has been implicated in several clinically relevant human conditions such as transplant rejection, rheumatoid arthritis, lupus, and T-cell lymphomas. PNP is therefore a target for inhibitor development aiming at T-cell immune response modulation and has been submitted to extensive structure-based drug design. The present analysis confirms the trimeric structure observed in the crystal. The potential application of the present procedure to other systems is discussed.
© 2003 Elsevier Inc. All rights reserved.

Keywords: Geometric docking; SAXS; Purine nucleoside phosphorylase; Bioinformatics

Recent developments in the algorithm for protein docking allowed the prediction of the conformation of quaternary structures of several proteins. Among all available algorithms for docking of biological macromolecules the geometric docking has been proved to generate reasonable models of several macromolecular assemblies [1,2]. Small angle X-ray scattering (SAXS) technique provides information on the structural characteristics of macromolecules in solution at a superatomic scale. One of the procedures to obtain structural information from SAXS results is based on the comparison between structure functions of proposed models with different configurations of monomers or subdomains with those determined from experiments. Even though this technique cannot guarantee the uniqueness of the model, it is widely used and was demonstrated to yield useful information on the structure, on structural variations, and on the quaternary structure of a number of macromolecules of biological interest [3]. The Guinier analysis of SAXS intensity provides a structural parameter, the radius of gyration of the macromolecule in solution, which is independent of any a priori model. The SAXS method also yields information on the spatial configuration of the macromolecular subdomains but ignores internal structural details and dynamics features such as, vibration, rotation or internal conformational changes [4].

Purine nucleoside phosphorylase (PNP) catalyzes the reversible phosphorolysis of the ribonucleosides and

* Corresponding author. Fax: +55-17-221-2247.
E-mail address: walterfa@df.ibilce.unesp.br (W.F. de Azevedo Jr.).

0006-291X/$ - see front matter © 2003 Elsevier Inc. All rights reserved.
doi:10.1016/j.bbrc.2003.08.093

2′-deoxyribonucleosides of guanine, hypoxanthine, and a number of related nucleoside compounds [5], except adenosine. Human PNP is an attractive target for drug design and it has been submitted to extensive structure-based design. PNP inhibitors could be used in the following applications: (1) treatment of T-cell leukemia; (2) suppression of the host versus graft response in organ transplantation recipients; (3) treatment of secondary or xanthine gout by restricting purine catabolites to the more soluble nucleosides; and (4) in combination with nucleosides to prevent their degradation by PNP metabolism [6]. More recently, the structure of human PNP has been solved using cryocrystallographic techniques at 2.3 Å resolution, which allowed a redefinition of the residues involved in the substrate binding sites [7,8]. The crystallographic structure is a trimer, however, there is a report of dimeric structure for the human enzyme [9], which may change the subunit interface. Since the active site is located near the interface of two subunits, changing the putative interactions between enzyme and inhibitors should have a bearing on structure-based inhibitor design.

Here we report the combination of geometric docking simulations and SAXS studies to assess the human PNP quaternary structure in solution. The general procedure, here described, may be used to study the spatial configuration of the macromolecular subdomains of other proteins in solution.

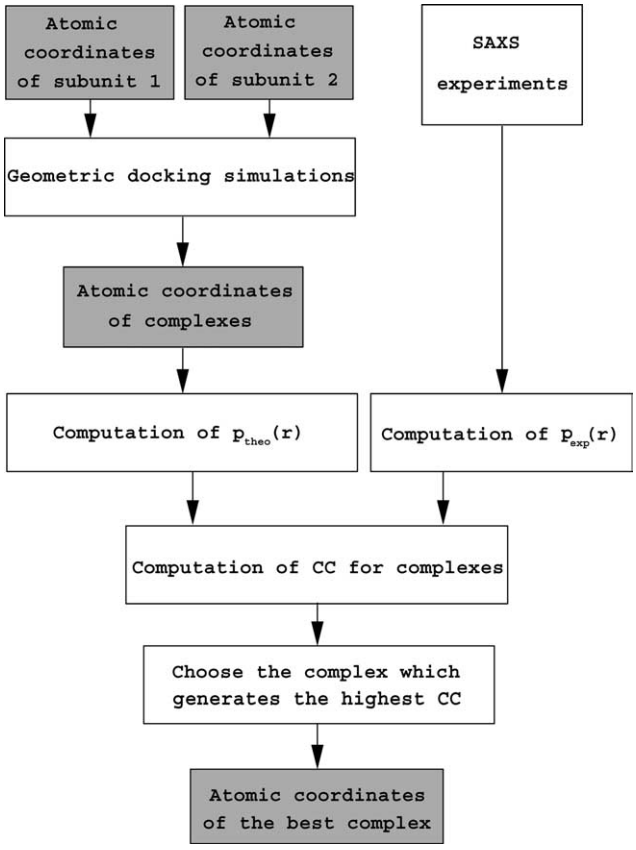

Fig. 1. Flowchart describing the overall strategy to assess protein complex conformations.

Materials and methods

Integration of geometric docking simulation and SAXS experiments. In order to assess the quaternary structure of PNP a scheme was used that involved both geometric docking simulations and SAXS experiments. A flowchart describing the overall strategy is shown in Fig. 1. This procedure was used to generate the dimeric models for PNP and the trimeric structure was built using the crystallographic symmetry. In order to speed up the geometric docking simulations, a parallel version of the program GRAMM [10] was used to generate the dimeric models for human PNP. Each step of the procedure is described in the following sections.

Geometric docking simulations. In order to obtain the dimeric structure of human PNP, docking simulation was performed using the geometric recognition algorithm, which was developed to identify molecular surface complementarity. The monomeric structure of human PNP (PDB access code: 1M73) [7] was docked against its own structure. It generated a total of 100 dimers. The geometric recognition algorithm is based on a geometrical approach and involves an automated procedure including: (i) a digital representation of the molecules by three-dimensional discrete functions; (ii) the calculation of a correlation function that assesses the degree of molecular surface overlap and penetration upon relative shifts of the molecules in three dimensions; and (iii) a scan of the relative orientations of the molecules [10]. The procedure is equivalent to a six-dimensional search but considerably faster by design, and the computation time is only moderately dependent on molecular size. This procedure has been applied to assess protein–protein and protein–ligand interactions. The geometric recognition algorithm was implemented in the program GRAMM [10]. All geometric docking simulations were performed on a Beowulf cluster, with 16 nodes (B16/AMD Athlon 1800+; BioComp, São José do Rio Preto, SP, Brazil).

SAXS studies. X-ray scattering data were collected at room temperature using Cu Kα X-rays radiation generated by a Rigaku RU300 rotating anode generator operated at 50 kV and 90 mA and collimated with a block slit system [11]. The scattering intensity was measured using a linear position sensitive detector (CBPF-Brazil).

The SAXS measurements were performed within an angular range defined by $0.02\,\text{Å}^{-1} < h < 0.450\,\text{Å}^{-1}$ where $h = (4\pi\sin)/\lambda$, 2θ being the angle between the incident and the scattered X-ray beam and λ the X-ray wavelength. The contributions to the scattering intensity from the solvent, capillary, and air were subtracted from the total intensity.

Recombinant human PNP was expressed and purified as previously described [12]. The SAXS measurements were carried out using human PNP solution, which was concentrated to 12 mg ml^{-1} against 10 mM potassium phosphate buffer (pH 7.1). The counting time was 12 h. The extrapolated experimental SAXS intensity function was desmeared to suppress the influence from the slit collimation system yielding the corrected intensities, $I(h)$.

A structural parameter related to the overall size of the macromolecule, the radius of gyration R_g, was determined by using the Guinier equation [13]

$$I(h) = I(0)\exp\left[-\frac{h^2R_g^2}{3}\right]. \quad (1)$$

Eq. (1) applies to macromolecules in the limits of a dilute solution and small h values. More detailed information of the molecular structure can be obtained from the distance distribution function $p(r)$, which is related to the SAXS desmeared (free from geometrical collimation effects) intensity $I(h)$ by

$$p(r) = \frac{1}{2\pi^2}\int_0^\infty I(h)(hr)\sin(hr)\,\mathrm{d}h. \quad (2)$$

The $p(r)$ function is proportional to the number of pairs of electrons separated by the distance r, which is encountered by combinations between all the elements of the macromolecule. The radius of gyration of macromolecules in solution is usually determined by applying Eq. (1). The distance distribution function, $p_{\exp}(r)$, has been determined by indirect Fourier transformation using the ITP program [11]. This program was also used to determine the intensity $I(h)$, free from smearing collimation effects. The theoretical function $p_{\text{theo}}(r)$ was calculated using the program MULTIBODY [11], modified in order to make molecular model building easier [4]. The program MULTIBODY calculates the resulting function $p(r)$ of the complete set of atomic coordinates of each structural model for the macromolecule. In the present study we calculated the $p_{\text{theo}}(r)$ for monomer, for the dimers, generated by geometric docking, and for the trimer, obtained by application of crystallographic rotations.

Correlation between geometric docking simulations and SAXS experiments. To assess the correlation between theoretical and experimental distance distribution function $p_{\exp}(r)$ and $p_{\text{theo}}(r)$, respectively, we have calculated the linear correlation coefficient (CC), which is defined as follows [14]:

$$\mathrm{CC} = \frac{\sum_i^n \left[\left(|p_{\exp,i}(r)|^2 - \overline{|p_{\exp}(r)|^2}\right) \times \left(|p_{\text{theo,i}}(r)|^2 - \overline{|p_{\text{theo}}(r)|^2}\right)\right]}{\left[\sum_i^n \left(|p_{\exp,i}(r)|^2 - \overline{|p_{\exp}(r)|^2}\right)^2 \sum_i^n \left(|p_{\text{theo,i}}(r)|^2 - \overline{|p_{\text{theo}}(r)|^2}\right)^2\right]^{\frac{1}{2}}}, \quad (3)$$

where $\overline{|p_{\exp}(r)|^2}$ is the mean of the $|p_{\exp,i}(r)|^2$, $\overline{|p_{\text{theo}}(r)|^2}$ is the mean of $|p_{\text{theo,i}}(r)|^2$, and sums are made over all available $p(r)$. When a correlation is known to be significant, CC is one conventional way of summarizing its strength. The complex, which generates the highest correlation coefficient, is considered the right macromolecular conformation. In the present work, we calculated the CC for all dimeric models obtained from the geometric docking simulations and for the monomeric and trimeric structures.

Results and discussion

Guinier plot ($\log I(h)$ versus h^2) of the desmeared scattering function is displayed in Fig. 2. The slope of linear portion of this plot was determined to obtain the radius of gyration of human PNP. The R_g value was 29.8 Å.

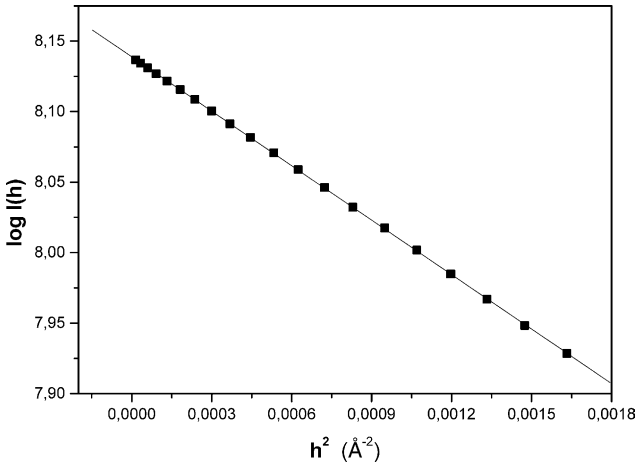

Fig. 2. Guinier plot of the SAXS intensities, $I(h)$, for human PNP. The straight line was obtained by least-squares fitting in the region $h^2 < 1.8.10^{-3}$ Å^2.

PNPs from most mammalian and some of the bacterial sources appear to be trimeric although dimeric quaternary structures have been proposed for the human enzyme [9]. Analysis of the crystallographic structures of human PNP indicates a trimeric structure (PDB access codes: 1ULA, 1ULB, 1M73, and 1PWY) [6–8,15]. However, in a number of instances the quaternary structure observed in the crystalline state is not conserved in solution [3]. Furthermore, in the case of human PNP the low pH used in the crystallization condition [16] may generate differences in the spatial configuration of the macromolecular subdomains observed in the crystal when compared to the structure in physiological pH. In addition, since the active site of the PNP is located near the interface of two subunits within the trimer, the precise information about the biological unit in solution is of capital importance to guide the structure-based design of inhibitors because its target is a structure as close as possible to the structure found in the physiological conditions, where the drug will act. Up to now all structure-based designs of PNP inhibitors have used the low-resolution structures of human PNP (PDB access codes: 1ULA and 1ULB) and consider the trimer as the target for molecular modeling studies.

Three families of theoretical models, based on the high-resolution crystallographic structure (PDB access code: 1M73) [7], were used to determine the theoretical distance distribution function, $p_{\text{theo}}(r)$, using the program MULTIBODY and then compared with the experimental function $p(r)$ determined using the ITP program from SAXS data. Figs. 3A–C show structural models and the experimental distribution function against the theoretical distribution function for the monomer, dimer, and trimer, of human PNP, respectively.

The atomic coordinates for monomeric structure were obtained from the asymmetric unit content of the crystallographic structure of human PNP solved at 2.3 Å resolution [7]. Previous statistical analysis of low-resolution docking indicated that gross structural features of protein–protein interactions could be identified for a significant percentage of protein complexes [1]. Therefore, the low-resolution protocol of the GRAMM program [10] was used to generate the dimeric models. A total of 100 models for the dimeric structure were built, only the complex, which generated the highest correlation coefficient between theoretical and experimental distance distribution function is shown in Fig. 3B. The trimeric structure was built applying two successive rotations of 120° along z-axis on the atomic coordinates of the monomer. The radii of gyration for the structural models are 18.7, 26.5, and 28.7 Å, for the monomer, dimer, and trimer, respectively.

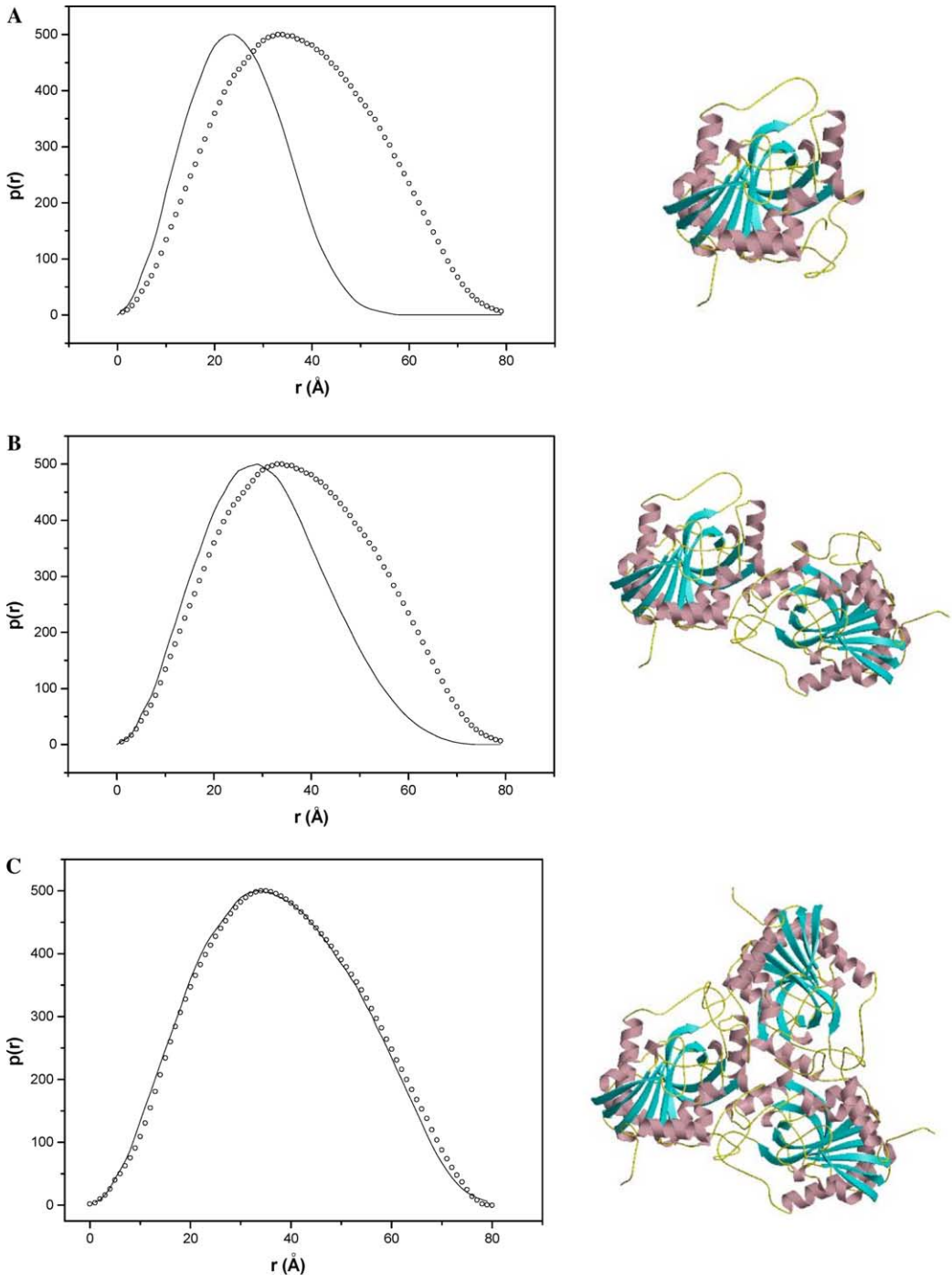

Fig. 3. Proposed structural models for human PNP and the corresponding theoretical (continuous line) and experimental (dotted line) distance distribution functions, $p(r)$, for: (A) monomer, (B) dimer, and (C) trimer. The model figures were generated by MOLSCRIPT [27] and Raster3D [28].

The value CC lies between −1 and 1. It has a value of 1, when the data points lie on a perfect straight line with positive slope. If the data points lie on a perfect straight line with negative slope, then CC has the value −1 [14]. The correlation coefficient between theoretical and experimental distance distribution functions ranges from 0.591 to 0.995, and the highest correlation coefficient was obtained for the trimeric structure, which also presented the radius of gyration closer to the experimental radius of gyration.

The contact area at interface between each subunit in the PNP trimer is 1124 $Å^2$, which indicates that the subunits are strongly bound to each other. Fig. 4 shows the electrostatic potential surface at subunit interface of the trimeric structure generated using GRASP [17]. Analysis of the electrostatic potential surface at the

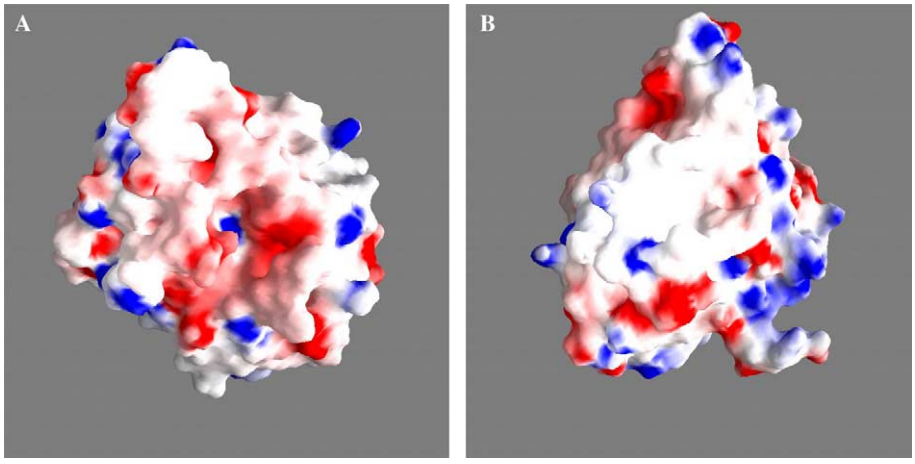

Fig. 4. Electrostatic potential surface at subunit interface of human PNP, calculated with GRASP [17] and shown from −10 to +10 kT. Uncharged regions are white.

subunit interface indicates good shape complementarity and some charge complementarity; however, most of the contacts are hydrophobic and involve residues Tyr88, Phe141, Phe159, Phe200, and Leu209.

The trimeric PNP structure has been extensively used for structure-based studies of PNP inhibitors [5,6,18–25]. However, the quaternary structure of human PNP in solution and in physiological pH has not been previously investigated using low-resolution methods, such as SAXS. The present analysis of the SAXS experiments integrated with geometric docking simulation strongly indicates that human PNP is a trimer in solution, the agreement found between the experimental and theoretical $p(r)$ functions for the trimer suggests that structure in solution adopts approximately the same conformation identified in the high-resolution crystallographic structure (PDB access code: 1M73) [7]. The radius of gyration determined for the trimeric structure is slightly smaller than that determined from the Guinier plot ($\log I(h)$ versus h^2) of the desmeared scattering function. The possible reasons for this discrepancy may be the cryogenic conditions used to solve the high-resolution structure of human PNP and the absence of solvents in the theoretical model.

The integration of a high-efficient algorithm for geometric docking with SAXS experiments allowed the investigation of the possible quaternary structures not observed in the crystalline state, such as the putative PNP dimeric structure [9]. The procedure adopted to analyze the interaction between PNP subunits can be used for other protein complexes. The main applications of the present methodology are: (1) analysis of interactions between biological macromolecules using structural models obtained from crystallography or NMR, (2) validation of structural models obtained from molecular modeling [26] of complexes of biological macromolecules, and (3) analysis of complexes of biological macromolecules in conditions closer to the biological environment.

Geometric docking simulations may be omitted from the strategy if the atomic coordinates for the complexes are available. We are applying the procedure, here described, to assess the quaternary structure of a number of protein complexes, such as hemoglobins, PNPs, and crotoxin.

Acknowledgments

This work was supported by grants from FAPESP (SMOLBNet, Proc. Num. 01/07532-0), CNPq, CAPES and Instituto do Millenium (CNPq-MCT). W.F.A. (CNPq, 300851/98-7), M.S.P. (CNPq, 500079/90-0), and L.A.B. (CNPq, 520182/99-5) are researchers for the Brazilian Council for Scientific and Technological Development.

References

[1] A. Tovchigrechko, C.A. Wells, I.A. Vakser, Docking of protein models, Protein Sci. 11 (2002) 1888–1896.
[2] N. Jing, C. Marchand, J. Liu, R. Mitra, M.E. Hogan, Y. Pommier, Mechanism of inhibition of HIV-1 integrase by G-tetrad-forming oligonucleotides in vitro, J. Biol. Chem. 275 (2000) 21460–21467.
[3] D.I. Svergun, C. Barberato, M.H.J. Koch, L. Fetler, P. Vachette, Large differences are observed between the crystal and solution quaternary structures of allosteric aspartate transcarbamylase in the R state, Proteins Struct. Funct. Genet. 27 (1997) 110–117.
[4] J.R. Olivieri, A.F. Craievich, The subdomain structure of human serum albumin in solution under different pH conditions studied by small angle X-ray scattering, Eur. Biophys. J. 24 (1995) 77–84.
[5] J.A. Montgomery, Purine nucleoside phosphorylase: a target for drug design, Med. Res. Rev. 13 (1993) 209–228.
[6] S.E. Ealick, Y.S. Babu, C.E. Bugg, M.D. Erion, W.C. Guida, J.A. Montgomery, J.A. Secrist III, Application of crystallographic and modeling methods in the design of purine nucleoside phosphorylase inhibitors, Proc. Natl. Acad. Sci. USA 91 (1991) 11540–11544.

[7] W.F. de Azevedo Jr., F. Canduri, D.M. Santos, R.G. Silva, J.S. Oliveira, L.P.S. Carvalho, L.A. Basso, M.A. Mendes, M.S. Palma, D.S. Santos, Crystal structure of human purine nucleoside phosphorylase at 2.3 Å resolution, Biochem. Biophys. Res. Commun. 308 (2003) 545–552.
[8] D.M. Santos, F. Canduri, J.H. Pereira, M.V.B. Dias, R.G. Silva, M.A. Mendes, M.S. Palma, L.A. Basso, W.F. de Azevedo, D.S. Santos, Crystal structure of human purine nucleoside phosphorylase complexed with acyclovir, Biochem. Biophys. Res. Commun. 308 (2003) 553–559.
[9] A.S. Lewis, B.A. Lowy, Human erythrocytes purine nucleoside phosphorylase: molecular weight and physical properties, J. Biol. Chem. 254 (1979) 9927–9932.
[10] E. Katchalski-Katzir, I. Shariv, M. Eisenstein, A.A. Friesem, C. Aflalo, I.A. Vakser, Molecular surface recognition: determination of geometric fit between proteins and their ligands by correlation techniques, Proc. Natl. Acad. Sci. USA 89 (1992) 2195–2199.
[11] O. Glatter, in: O. Glatter, O. Kratky (Eds.), Small Angle X-Ray Scattering, Academic Press, London, 1982.
[12] R.G. Silva, L.P. Carvalho, J.S. Oliveira, C.A. Pinto, M.A. Mendes, M.S. Palma, L.A. Basso, D.S. Santos, Cloning, overexpression, and purification of functional human purine nucleoside phosphorylase, Protein Expr. Purif. 27 (2003) 158–164.
[13] A. Guinier, G. Fournet, Small-Angle Scattering of X-rays, Wiley, New York, 1955.
[14] W.H. Press, S.A. Teukolsky, W.T. Vetterling, B.P. Flannery, Numerical Recipes in FORTRAN. The Art of Scientific Computing, second ed., Cambridge University Press, New York, 1992.
[15] S.E. Ealick, S.A. Rule, D.C. Carter, T.J. Greenhough, V. Babu, W.J. Cook, J. Habash, J.R. Helliwell, J.D. Stoeckler, R.E. Parks Jr., F. Chen, C.E. Bugg, Three-dimensional structure of human erythrocytic purine nucleoside phosphorylase at 3.2 Å resolution, J. Biol. Chem. 265 (1990) 1812–1820.
[16] W.J. Cook, S.E. Ealick, C.E. Bugg, J.D. Stoeckler, R.E. Parks Jr., Crystallization and preliminary X-ray investigation of human erythrocytic purine nucleoside phosphorylase, J. Biol. Chem. 256 (1981) 4079–4080.
[17] A. Nicholls, K. Sharp, B. Honig, Protein folding and association: insights from the interfacial and thermodynamic properties of hydrocarbons, Proteins Struct. Funct. Genet. 11 (1991) 281–296.
[18] P.W.K. Woo, C.R. Kostlan, J.C. Sircar, M.K. Dong, R.B. Gilbertsen, Inhibitors of human purine nucleoside phosphorylase. Synthesis and biological activities of 8-amino-3-benzylhypoxanthine and related analogues, J. Med. Chem. 35 (1992) 1451–1457.
[19] J.-W. Chern, H.-Y. Lee, C.-S. Chen, Nucleosides. 5. Synthesis of guanine and formycin B derivatives as potential inhibitors of purine nucleoside phosphorylase, J. Med. Chem. 36 (1993) 1024–1031.
[20] M.D. Erion, S. Niwas, J.D. Rose, S. Ananthan, M. Allen, J.A. Secrist III, Y.S. Babu, C.E. Bugg, W.C. Guida, S.E. Ealick, J.A. Montgomery, Structure-based design of inhibitors of purine nucleoside phosphorylase. 3. 9-Arylmethyl derivatives of 9-deazaguanine substituted on the methylene group, J. Med. Chem. 36 (1993) 3771–3783.
[21] J.A. Secrist III, S. Niwas, J.D. Rose, Y.S. Babu, C.E. Bugg, M.D. Erion, W.C. Guida, S.E. Ealick, J.A. Montgomery, Structure-based design of inhibitors of purine nucleoside phosphorylase. 2. 9-Alicyclic and 9-heteroalicyclic derivatives of 9-deazaguanine, J. Med. Chem. 36 (1993) 1847–1854.
[22] W.C. Guida, R.D. Elliot, H.J. Thomas, J.A. Secrist III, Y.S. Babu, C.E. Bugg, M.D. Erion, S.E. Ealick, J.A. Montgomery, Structure-based design of inhibitors of purine nucleoside phosphorylase. 4. A study of phosphate mimics, J. Med. Chem. 37 (1994) 1109–1114.
[23] S. Niwas, P. Chand, V.P. Pathak, J.A. Montgomery, Structure-based design of inhibitors of purine nucleoside phosphorylase. 5. 9-Deazahypoxanthines, J. Med. Chem. 37 (1994) 2477–2480.
[24] P.E. Morris, A.J. Elliott, S.P. Walton, C.H. Williams, J.A. Montgomery, Synthesis and biological activity of a novel class of purine nucleoside phosphorylase inhibitors, Nucleosides Nucleotides Nucleic Acids 19 (2000) 379–404.
[25] A. Andricopulo, R.A. Yunes, Structure–activity relationships for a collection of structurally diverse inhibitors of purine nucleoside phosphorylase, Chem. Pharm. Bull. 49 (2001) 10–17.
[26] A. Sali, T.L. Blundell, Comparative protein modelling by satisfaction of spatial restraints, J. Mol. Biol. 234 (1993) 779–815.
[27] P.J. Kraulis, MOLSCRIPT: a program to produce both detailed and schematic plots of proteins, J. Appl. Cryst. 24 (1991) 946–950.
[28] E.A. Merritt, D.J. Bacon, Raster3D: photorealistic molecular graphics, Methods Enzimol. 277 (1997) 505–524.